




Research Article

A novel optimized design of a piezoelectric-driven 4-stage amplified compliant microgripper using a 2-step multi-objective algorithm

Hamid Haghshenas Gorgani¹  · Sharif Shabani² · Mohammadmahdi Honarmand²

Received: 30 December 2021 / Accepted: 3 March 2022

Published online: 28 March 2022

© The Author(s) 2022 

Abstract

Advancements in microscale technologies have prompted a demand for high precision micro-manipulation. Microgrippers are the primary means of conducting micro-scale operations, and they significantly affect the procedure's performance. This paper presents a novel optimized design for compliant microgrippers, intending to enhance functionality and durability. The mainframe of the proposed microgripper is based on a compact flexure-based compliant structure with four stages of movement amplification. Experiments were designed based on the L25 Taguchi orthogonal arrays. The experiments were conducted using the finite element method in Abaqus 6.14 workbench. Range of motion and maximum created mechanical stress are selected as the two fundamental goals of the optimization. A variety of designs are achieved using the proposed algorithm. The use of Analytical Hierarchy Process has led to the presentation of an efficient and well-defined algorithm to perform decisions. The decision process can be performed with regard to specific requirements of various applications. The presented design process of microgrippers has the potential for customized manufacturing for specific applications.

Article Highlights

- Finding correlations between design parameters and outputs (Amplification factor & Stress), using Taguchi's method in design of experiments (DOE).
- Optimization of dimensional inputs using a multi-objective genetic algorithm process to achieve an optimal Pareto-front instead of a single design point.
- Selecting the desirable point on the optimal Pareto-front for specific applications using Analytic Hierarchy Process (AHP) to prevent possible decision-making errors.

Keywords Microgripper · Compliant mechanism · Multi-stage amplification · Non-dominated sorting genetic algorithm (NSGA-II) · Multi-objective optimization

1 Introduction

In the last decades, the rapid development of Micro-electromechanical systems (MEMS) has raised global interest in micro-operations, which are used in a wide variety of applications such as bioengineering [1], drug delivery [2], optics [3], and aerospace [4]. As the importance and

applications of manipulating small parts and objects increase, instruments, and tools for carrying out such operations are becoming of great favor to scientists.

Microgrippers are used to carry out micro-scale operations with the desired precision. Using a flexible mechanism in the microgripper lowers the manufacturing costs

✉ Hamid Haghshenas Gorgani, h_haghshenas@sharif.edu | ¹Engineering Graphics Center, Sharif University of Technology, Tehran, Iran. ²Department of Mechanical Engineering, Sharif University of Technology, Tehran, Iran.



and omits friction, clearance, and the need for lubrication [5].

Common actuation mechanisms to achieve the desired motion of interest in microgrippers include electrothermal [6, 7], electrostatic [8], pneumatic [9], electromagnetic [10], shaped memory alloy [11, 12], and piezoelectric actuators [13, 14]. Voice Coil Motors (VCM) have been used to create extensive ranges of motion in micro/nano-positioning mechanisms while delivering a high speed of motion [15, 16].

Comparing to other types of actuation, piezoelectric stack actuators have advantages such as fast response, high resolution, stable displacement and large output force [17, 18].

The output displacement of piezo-electric stack actuators is usually much smaller than the size of objects we aim to manipulate.

Displacement amplification mechanisms have been utilized to amplify the input displacement of microgrippers, resulting in a greater range of motion in the gripping jaws [19].

Due to various features expected of Microgrippers, some studies operated a multi-objective optimization on its design. Dao et al. [20] performed a multi-objective optimization based on displacement and frequency. They achieved a set of optimal dimensions using the differential evolution algorithm. Ho et al. [21] performed an optimization based on hybrid Taguchi-teaching learning-based optimization algorithm (HTLBO) choosing displacement, frequency and gripping effort as objectives. Xiao et al. [22] derived an optimal design of microgripper, based on input stiffness, safety factor and amplifier ratio. Using Radius basis functional network (RBFN) multi-objective GA (Genetic Algorithm) optimization method, they derived a set of optimal designs. Ho et al. [23] carried out an optimization using hybridization algorithm between adaptive neuro-fuzzy inference system (ANFIS) and Jaya algorithm in order to achieve an optimal displacement and resonance frequency. Grossard et al. [24] performed a flexible building block method optimization on microgripper to achieve a higher stroke amplification and force amplification. Nguyen et al. [25] optimized a sand crab-inspired compliant microgripper based on the amplification factor and the maximum stress created by a specific displacement. Das et al. [26] used computational methods to optimize a piezoelectric microgripper design to minimize parasitic motion and increase output displacement. Their experimental results demonstrated low parasitic motion and high precision motion resolution of their microgripper.

Based on what has been said, an overview of the literature shows three major weaknesses:

First, due to the use of the full factorial method, the number of experiments to achieve the desired result will be very large. This is a complicated matter in cases involving theoretical analysis and costly and time consuming when conducting practical experiments.

Second, most research has done the process of optimizing the micro-gripper to reach a design point. But due to the wide range of applications of microgrippers, we will need different outputs. For example, sometimes we need to withstand high stress and sometimes a large amplification factor. Therefore, instead of achieving a single design point, it is better for the user to have a set of designs so that he/she can choose the desired design point according to his/her needs.

Third, in cases where the choice of the desired design point is left to the user, unsystematically doing of the selection process leads to decision errors due to incorrect feeling of the demands. Therefore, using a systematic multi-criteria decision-making process is necessary to solve this problem. Of course, this in itself can complicate the process. So, the decision-making method should be effective and simple at the same time.

To address the first weakness, experiments based on the full factorial method are replaced by the Taguchi orthogonal arrays, which, significantly reduce the volume of records while covering the entire data. In addition, to determine the correlation of the parameters, low effect values are eliminated and lead to a concise, agile, and effective regression equation.

For the second, instead of using single-objective optimization, a multi-objective meta-heuristic algorithm based on the genetic algorithm is used, and therefore a single optimal point is replaced by an optimal Pareto-front that provides output flexibility for different applications.

To solve the third problem, the "Analytical Hierarchy process" (AHP), which is a multi-criteria decision-making method, allows the systematic selection of the desired design point according to the real expectations of the user based on the matrix of pairwise comparisons.

It is important to note that the focus of this research is not on a specific design or specific output parameters, but is to provide a fast, flexible and efficient algorithm, yet simple and low cost to optimize the parameters of a microgripper. Therefore, the selected outputs such as amplification factor, stress, vibration modes, dynamic or thermal considerations etc., the method of identification of correlations and validation is not important and done only using the finite element method. Of course, this algorithm can be generalized to the experimental data.

In this research, we present two important factors of a microgripper design, which can help us choose a design for our specific kind of application. These two factors are the amplification factor (AF) and minimal stress. For a set

of designs that have the same overall structure but vary in some features, there is usually a tradeoff between these two factors. When we increase the amplification factor, we observe an increase in the maximum stress created in the design and vice versa. Therefore, in this study, a novel method of obtaining the right design for one's needs was developed, utilizing a multi-objective optimization procedure and an importance criterion. Using this criterion, one can decide the relative importance of amplification factor and minimal stress, which will help choose the right design. This method of having minor variations in designs and choosing from them becomes especially important since for every design, achieving a well-regulated control system needs a lot of experiment and design knowledge. However, if we use a universal design with minor regulations to our work, we already know how to best control it and where to put our sensors. Flexibility and efficiency are expected from a universal design. As a result, having a great range of motion and easy means of producing movement were two important factors in our design. To ensure a great range of motion, we used four stages of amplification, and we achieved a remarkable magnitude of amplification factor.

This study aims to investigate the optimization of a four-stage microgripper based on the range of motion and stress responses. Following the introduction, the design process and the computational procedure used to perform the analyses are presented. Afterward, the design of experiments and the mathematical modelings are explained. Results are subsequently presented to demonstrate possible optimized designs. In addition, the observations on the experimental results are discussed further. Finally, conclusions are drawn based on the results and discussions.

2 Design of the microgripper and the finite element analysis

A main view diagram of the proposed microgripper is presented in Fig. 1. The microgripper is comprised of two stack piezoelectric ceramic actuators (SPCA), fixing holes, preload bolts, bridge amplifiers, lever amplifiers, a number of circular and rectangular flexure hinges, and finally, a pair of gripping jaws. By going through elastic deformation, flexure hinges transmit the produced displacements of the SPCAs to create the desired gripping motion. The symmetry of the structure improves accuracy, helps balance the structure's internal stress, and doubles the displacement amplification. Preload bolts are used to adjust the preload force on each SPCA. One end of each SPCA is fixed with the displacement transmission mechanism (DTM) using the preload bolt. Several fixing holes on the microgripper are used to keep the microgripper in place.

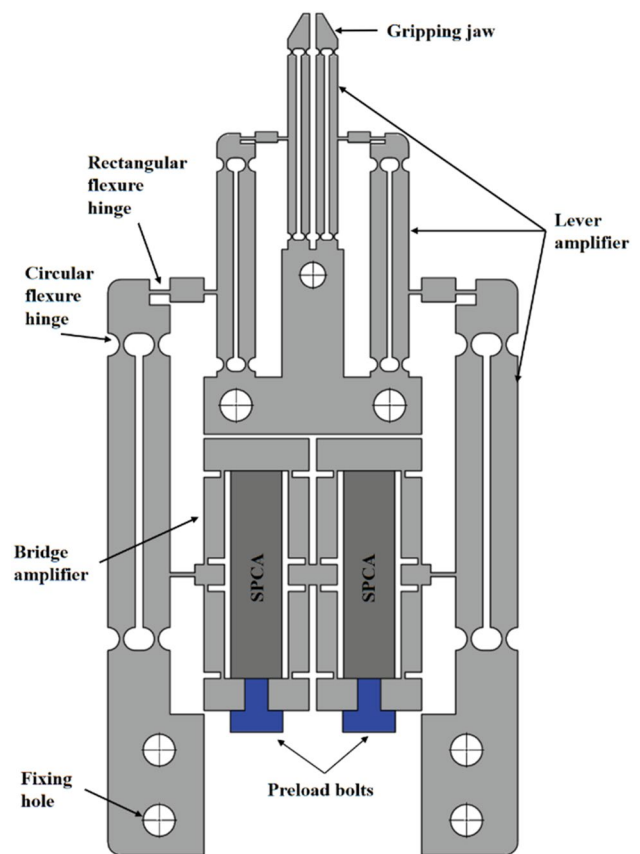


Fig. 1 Schematic diagram of the proposed microgripper

Figure 2 presents the main design parameters of the proposed microgripper design, which are also specified in Table 1.

The piezoelectric actuators produce a small output displacement; hence, four stages of displacement amplification were incorporated to ensure a great gripping stroke in the microgripper, leading to a large tip displacement. A bridge amplifier and three lever amplifiers were deployed to increase the output displacement.

Compliant mechanisms move solely by the deformation and flexure of hinges. Therefore, friction and unwanted motions are eliminated in compliant mechanisms. As a result, the microgripper's controlling system can possess a greater movement precision in such designs.

As for the material, the Aluminum alloy was used due to its favorable mechanical properties such as relatively low density, high flexibility, low cost, and being easy to be machined using electric discharge machining (EDM). Therefore, 7075 aluminum alloy was chosen, which has a modulus of elasticity $E = 71$ GPa, a Poisson's ratio $\nu = 0.33$, a yield strength $s = 455$ MPa, and a density $\rho = 2810$ kg/m³.

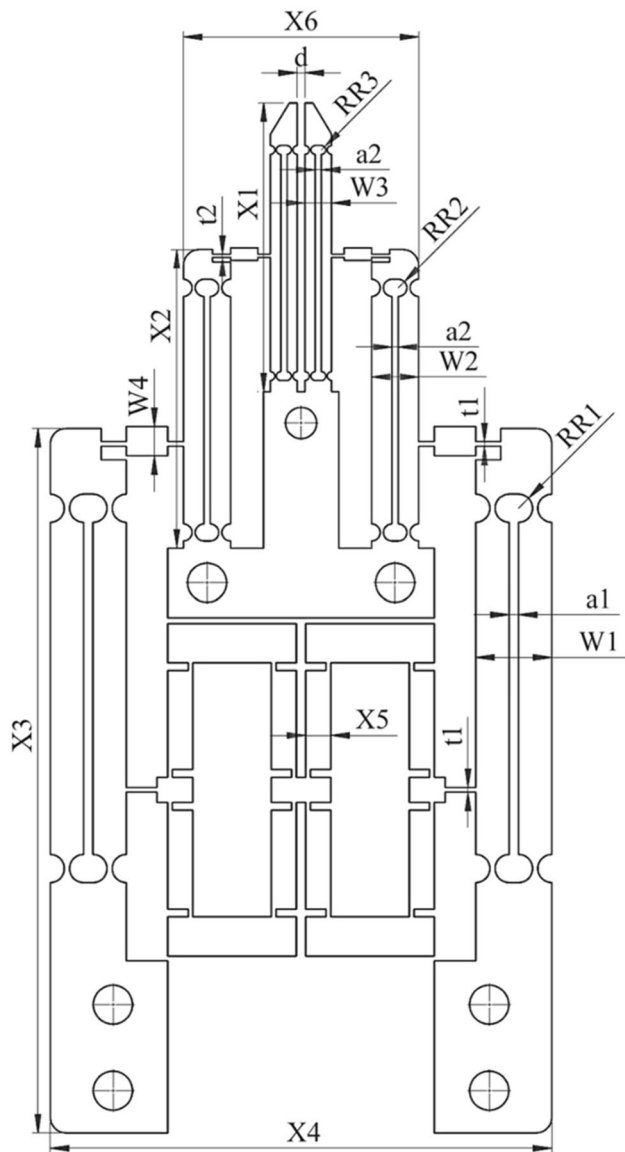


Fig. 2 Main design parameters of the proposed microgripper

Table 1 Main design parameters of the microgripper

Symbol	Value	Symbol	Value	Symbol	Value
X1	Var	X6	Var	W1	4.85
X2	Var	t1	0.3	W2	3
X3	Var	t2	0.2	W3	1.7
X4	Var	a1	0.6	W4	1.9
X5	Var	a2	0.4	Delta	0.5

In order to reduce the computational costs, a half-model was used in simulations, and an x-symmetric constraint was applied to the symmetry plane. A uniform distributed displacement in the y-direction was input to the

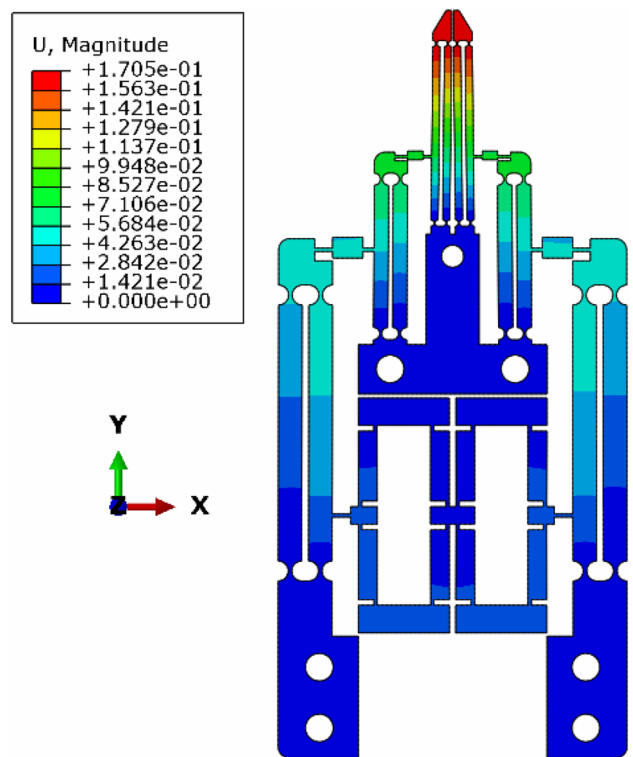


Fig. 3 FEA analysis diagram of the microgripper: displacement nephogram of microgripper

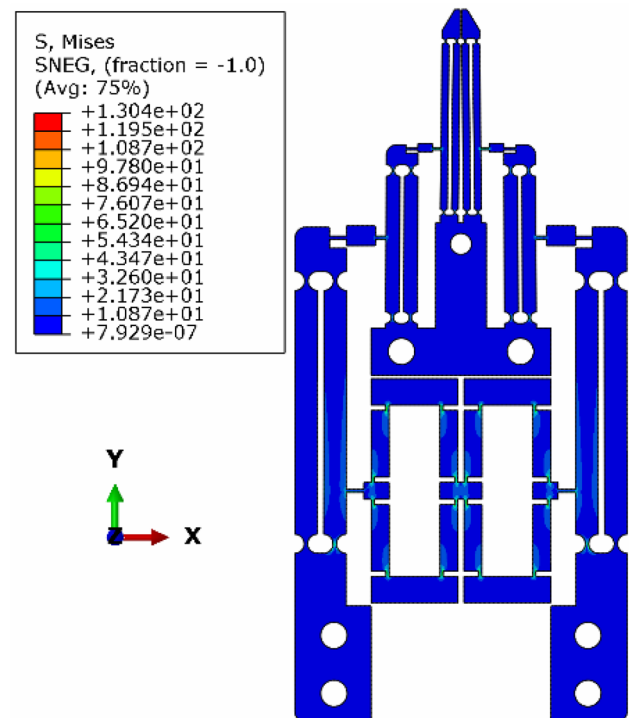


Fig. 4 FEA analysis diagram of the microgripper: stress nephogram of microgripper

Table 2 Comparison of the design of experiments by Taguchi orthogonal arrays with the full factorial method

Item	Taguchi Orthogonal Arrays	Full factorial	Comments
No. of the experiments	Few	A lot	Taguchi saves time and money
Ability to check qualitative or categorical variables	Yes	No	Wider range of practical applications for Taguchi
Study of variables at different levels	Yes	Yes	Full factorial can be more accurate
Ability to specify contributions for variables	Yes	Yes	Almost the same
Ability to estimate results in optimal conditions	Yes	Yes	Full factorial can be more accurate
The degree of complexity in the analysis	Simple	Very complicated	Using full factorial can lead to errors or take too long
Ability to estimate results at desired levels	Yes	Yes	Almost the same
Ability to perform multi-objective optimization	Yes (simple)	Yes (Very complicated)	Using full factorial can lead to fail, Errors or take too time

surfaces, which contact the upper and lower surfaces of the piezoelectric (5 μm in the "+y" direction for the upper surface and 5 μm in the "-y" direction for the lower surface). The surfaces of fixing holes were constrained to be fully encased. The displacement of gripping tips (which yields the amplification factor when divided by the input displacement of the piezoelectric) and the maximum stress generated in the microgripper structure were the outputs of the simulation. In order to mesh the samples, linear hexahedral elements of type C3D8R with a size of 0.04 mm were used, and a static-general solver with non-linear geometry was employed. A sensitivity analysis showed that a 0.04-mm mesh was fine enough to eliminate the effect of mesh size on the results. The contours of displacement and stress generated in the microgripper can be seen in Figs. 3 and 4.

3 Materials and methods

3.1 Design of experiments using the Taguchi method

The Taguchi method is one of the most powerful and stable methods of designing experiments. Comparing to the Full-Factorial method, the Taguchi method decreases the number of experiments in a drastic way, using orthogonal matrices [27]. The main advantage of the Taguchi method is to reduce price and time by decreasing the number of experiments, eliminating the effects of uncontrollable and noisy factors, and determining the main influencing factors [28, 29]. Furthermore, by this method, the interactions of factors on each other are identified. Table 2 compares the most important capabilities required in designing experiments using the Taguchi orthogonal array method with the full factorial

method. The Taguchi method can be summarized in the following steps:

1. Define the purpose of the study.
2. Define dependent variable (output).
3. Describe parameters affecting the output (independent variables).
4. Determine the levels of each of the independent variables and their validity range.
5. Select a suitable orthogonal matrix that is compatible with the number of variables and their levels.
6. Perform experiments according to the instructions obtained from the orthogonal matrix and record the results.
7. Analyze the results and implement the Taguchi algorithm based on signal to noise ratio and output interpretation.

An essential step in the Taguchi algorithm is defining the loss function, then defining the N/A relation function regarding the loss function [30]. The higher the signal-to-noise ratio, the higher the ratio of useful information to false information and noise [31]. Based on the nature of the dependent variable, the S/N ratio function can be defined in the following three ways [21–25, 27, 32–34]:

1. Smaller is better:

$$\frac{S}{N} = -10 \log \left(\frac{1}{n} \sum_{i=1}^n y_i^2 \right) \quad (1)$$

2. Larger is better:

$$\frac{S}{N} = -10 \log \left(\frac{1}{n} \sum_{i=1}^n \frac{1}{y_i^2} \right) \quad (2)$$

3. Nominal is better:

$$\frac{S}{N} = 10 \log \left(\frac{\bar{y}}{s_y^2} \right) \tag{3}$$

In these equations, Y_i is the i -th observation and n is the number of observations [32].

$$\bar{y} = \sum_{i=1}^n \frac{y_i}{n} \tag{4}$$

$$s_y^2 = \sum_{i=1}^n \frac{(y_i - \bar{y})^2}{n - 1} \tag{5}$$

Note that in all the above steps, a higher signal-to-noise ratio indicates that the variable has a stronger significant effect on the dependent variable than the misinformation and noise at the desired level. Also, the difference between the maximum and minimum signal-to-noise ratio at different levels for an independent variable represented by the " δ " parameter indicates that the variable has a greater effect on the output or the dependent variable [32].

3.2 Mathematical Modeling (Regression)

The collected data is analyzed by Minitab version 11 software. Different methods of regression can be used to model, predict and analyze various systems [25]. In this study, in order to find the relationship between the dependent variable and independent variables, first from Simple Linear Regression (SLR) and then Stepwise Linear Regression (SWLR) and then from Full Quadratic Linear Regression (FQMLR) and then Backward Full Quadratic Linear Regression (BFQMLR) is used to analyze the data. Then, using Analysis of Variance (ANOVA) parameters such as R^2 , Adjusted R^2 and Predict R^2 , also from P Value and finally RMSE, modeling methods are compared and the most accurate method is selected [35, 36]. The general equation for SLR is as follows:

$$y = \beta_0 + \beta_1 x + \epsilon \tag{6}$$

where x will be the predictor and β_0 and β_1 will be the model parameters (coefficients). Epsilon is a random component of the model that follows an independent normal distribution. The estimating equation of SLR method is as follows:

$$\hat{y} = b_0 + b_1 x \tag{7}$$

where b_0 and b_1 are the estimated parameters of the model and \hat{y} is the approximate value of the dependent variable y .

In SWLR method, effective parameters are added one after another while the ineffective parameter are removed on by one. The general and estimated equations of SWLR method are respectively as follows:

$$y = \beta_0 + \beta_1 x_i + \dots + \beta_j x_j + \epsilon \tag{8}$$

$$\hat{y} = b_0 + b_1 x_i + \dots + b_j x_j \tag{9}$$

where, x_i, \dots, x_j are the predictors and β_0, \dots, β_j are the model parameters. Also, b_0, \dots, b_j are the estimated model parameters and \hat{y} represents the approximate value of y .

Then FQMLR was used, the general equation of which is as follows [36, 37]:

$$y = \beta_0 + \beta_1 x_1 + \dots + \beta_k x_k + \beta_{1,1} x_1^2 + \dots + \beta_{k,k} x_k^2 + \beta_{1,2} x_1 x_2 + \dots + \beta_{k-1,k} x_{k-1} x_k \tag{10}$$

where, $\beta_0, \beta_1, \dots, \beta_k, \beta_{1,1}, \dots, \beta_{k,k}, \beta_{1,2}, \dots, \beta_{k-1,k}$ are model parameters (coefficients) and $x_1, x_1^2, \dots, x_k, x_k^2$ are the predictors.

The full-quadratic type of estimation equation MLR is as follows:

$$\hat{y} = b_0 + b_1 x_1 + \dots + b_k x_k + b_{1,1} x_1^2 + \dots + b_{k,k} x_k^2 + b_{1,2} x_1 x_2 + \dots + b_{k-1,k} x_{k-1} x_k \tag{11}$$

where, $b_0, b_1, \dots, b_k, b_{1,1}, \dots, b_{k,k}, b_{1,2}, \dots, b_{k-1,k}$ are estimations of model parameters and \hat{y} is the approximate predicted value of dependent variable(output). Then, to implement BFQMLR, in each step, each term of the FQMLR equation that has a P value > 0.05 is deemed as non-significant and is removed from Equation. Therefore, the final equation will have fewer parameters than FQMLR and at the same time will be more consistent with the data. Therefore, in the final comparison to choose the best method, it is enough to compare the ANOVA and Root Mean Square Error (RSME) analysis between SWLR and BFQMLR, and choose one of these two methods [35, 36].

3.3 Multi-objective Optimization Using NSGA-II:

The NSGA algorithm was first introduced in 1994 by Srinivas and Deb using the ranking and non-dominated sorting process [38]. This algorithm had problems in selecting higher quality individuals among all the individuals raised, problems in elitism and complexity of calculations. Therefore, in order to fix these problems, edited version was introduced in 2002 by Deb under the title NSGA-II [39]. Therefore, NSGA-II is an algorithm with high computational efficiency, fast, Non-elitism preventing, Non-Dominated Sorting, and with less control over shared members to maintain their diversity [34, 40–42].

The implementation steps of NSGA-II can be summarized as follows:

1. Generation of the initial population with size N and $\text{Gen}=0$
2. Calculation of all components of the objective function for all individuals of the initial population
3. Non-dominated sorting based on crowding distance and ranking
4. Selecting a portion of the initial population which have a higher ranking, generating crossover and mutation for making offspring
5. Making a new population with size $2N$ by a combination of parents and offspring populations
6. Rankin based on crowding distance and selecting N individuals with the higher rank
7. Checking end condition (it can be meet the maximum allowed generations, achieving the desired accuracy, reaching max. time limit and no improvement after in Maximum pre-defined number of generations).

The solution will consist of a set of points whose input are independent variables and whose output are all components of the objective function (dependent variables). Each point on optimal Pareto-front represents an optimal answer to the problem. It is clear that by changing one of the optimal output points, the other outputs will change. Therefore, it depends entirely on the selector will have to choose which point.

3.4 Optimum point Selection; An AHP Approach

There are several ways to select one of the several points on Optimal Pareto-front, all of which depend on the opinion of the selector. To ensure that the real and accurate opinion of the selector in determining the weight of each component of the objective function (dependent variables) is used in constructing the final output, a systematic method based on pairwise comparisons, called analytic hierarchical process, is used as the following [43]:

Suppose the number of dependent variables (output) is n , denoted by f_1 to f_n , in other words:

$$y = [f_1 \ f_2 \ \dots \ f_n] \quad (12)$$

In this case, we form a pairwise comparison matrix as follows:

$$A = \begin{bmatrix} 1 & a_{12} & \dots & a_{1n} \\ a_{21} & 1 & \dots & a_{2n} \\ \dots & \dots & \dots & \dots \\ a_{n1} & a_{n2} & \dots & 1 \end{bmatrix} = [a_{ij}] \quad (13)$$

Where a_{ij} represents the comparative significance of output f_i over output f_j , determined on a predetermined scale (usually from 1 to 5). It should be known that $a_{ii} = 1$ ($i : 1$ to n) and we have:

$$a_{ij} = \frac{1}{a_{ji}} \quad (14)$$

To calculate the weight of each output component we have:

$$W_i = \{a_{i1} \times a_{i2} \times \dots \times a_{in}\}^{\frac{1}{n}} \quad (15)$$

where W_i will be the weight of f_i . For normalized mode we have:

$$w_i^N = \frac{W_i}{\sum_{i=1}^n W_i} \quad (16)$$

where, w_i^N is the normalized weight of i -th output (or f_i).

Now for each row of optimal Pareto-front, the final combined output can be expressed as y_c and defined as below:

$$y_c = \sum_{i=1}^n w_i^N f_i \quad (17)$$

Now we just have to find the maximum value of calculated y_c values.

$$y_{\text{opt}} = \text{Max}(y_c) \quad (18)$$

Instead of multi-objective optimization mode, it is also possible to use a single-objective optimization mode with the following objective function from the beginning of the optimization process, and just find the optimum point:

$$\text{Objective function} : y_c = \sum_{i=1}^{\bar{n}} w_i f_i \quad (19)$$

3.5 The Proposed Algorithm

The proposed algorithm can be divided into two basic steps:

Modeling stage, Includes geometric designing of the microgripper, defining independent variables (inputs), defining dependent variables (outputs), design and execution of experiments based on proper definition and selection of Taguchi orthogonal matrices, recording and analyzing results and thus ranking and separating variables with specific effects against variables with uncertain effect or noise (and eliminating them in the process of making a mathematical model), deriving a mathematical model using regression in two different ways, ANOVA analysis and deciding on the appropriate model based on this analysis.

Optimization stage, includes defining the multi-component objective function, modifying the objective function based on the nature of the outputs (so that all need to be minimized), performing the NSGA-II algorithm and

obtaining the Optimal Pareto-front, making decisions Regarding the selection of final optimal points on the Optimal Pareto-front based on the weights obtained from performing pairwise comparisons, performing AHP and defining the combined objective function. A summary of these steps is shown in Figs. 5 and 6.

3.6 Uncertainties and Limitations

Regarding this fact that we often have to use the Taguchi orthogonal arrays instead of the full factorial method due to cost and time considerations on the one hand and the complexity of the calculations and (sometimes) qualitative variables, on the other hand, the weaknesses of this method may affect our research. This means that the accuracy of the constructed mathematical models may be reduced due to the omission or misinterpretation of the interaction of the variables or the small number of experiments and the discrete levels.

In the FEM, the choice of elements and mesh sizes, geometric parameters of the model, and mechanical properties of the model material can be the primary sources of uncertainty in this study.

To eliminate these shortcomings, the results should always be validated within an acceptable range by performing a sufficient number of tests.

4 Results

According to the proposed algorithm, the first step is the geometric design of the microgripper. According to the review of the articles mentioned in the introduction section, the proposed plan is as shown in Fig. 1.

Also, the geometric design variable parameters are X1 to X6, which are specified in Fig. 2. The minimum and maximum values as well as the levels of each variable are according to Table 3.

Also, the outputs (independent variables) as mentioned in Sect. 4.1 are amplification factor and stress, which are hereinafter referred to as AF and ST in this article. The ultimate goal is to reach the maximum AF and the minimum ST.

According to the independent variables (inputs), dependent variables (outputs) and their nature, the Taguchi orthogonal matrix will be 6 factors and each will have 5 levels of type L25 and according to Table 3.

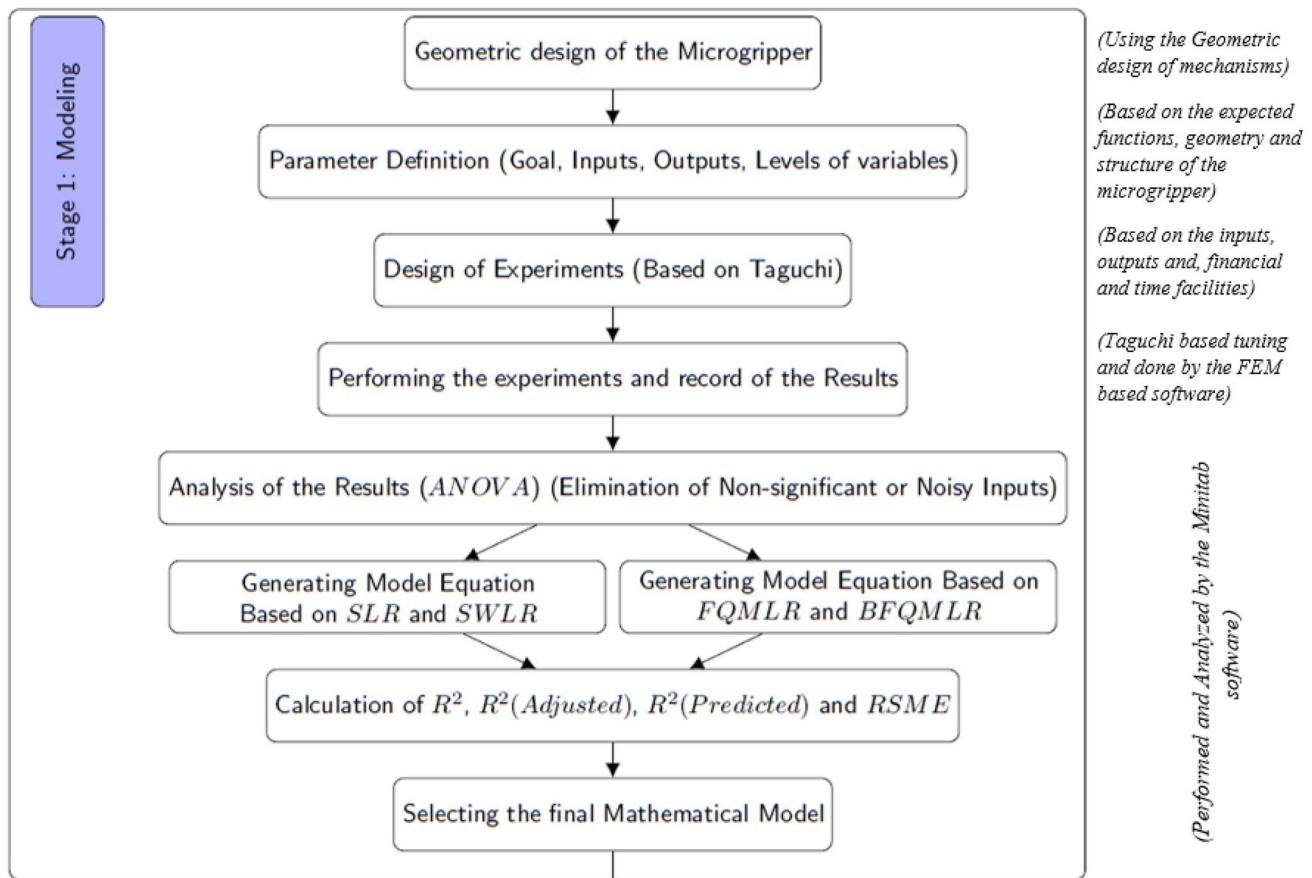


Fig. 5 Proposed optimization algorithm (stage1: modeling)

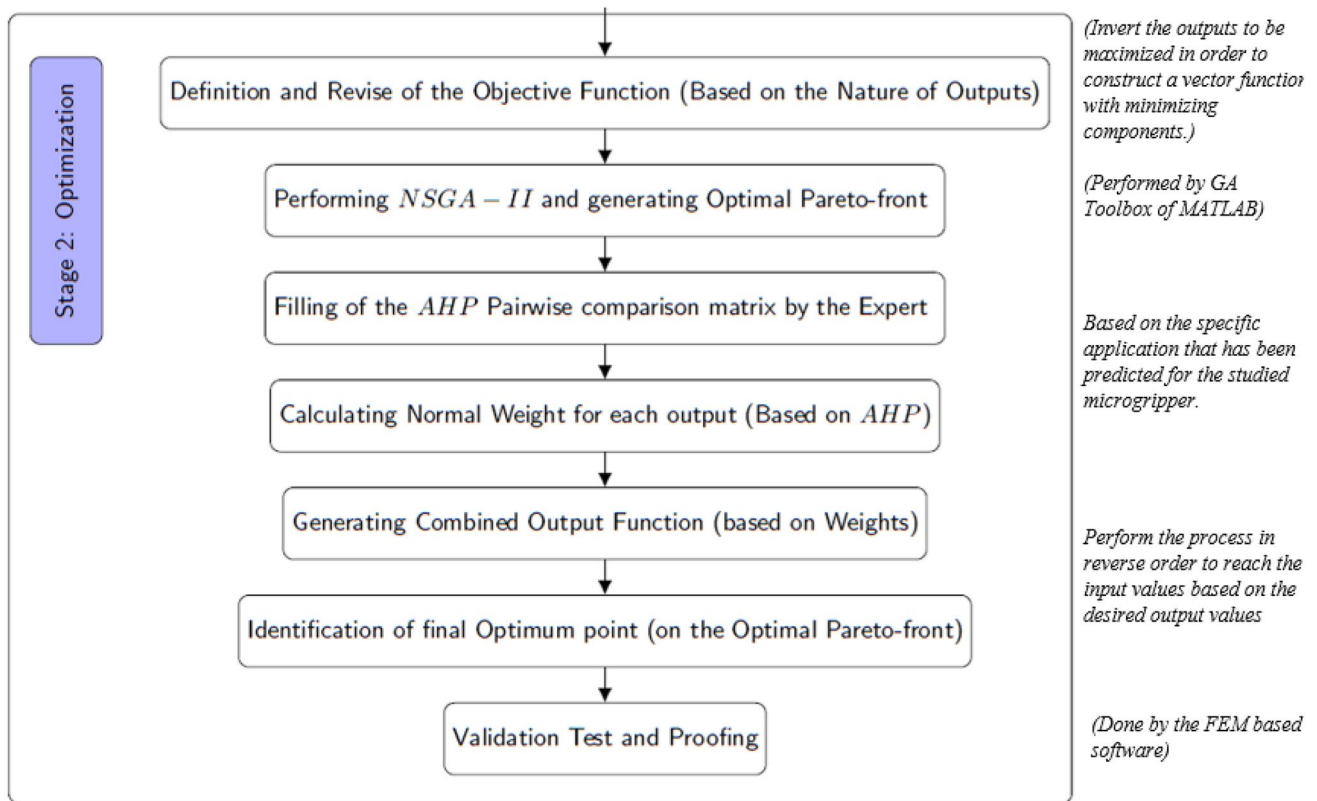


Fig. 6 Proposed optimization algorithm (stage2: optimization)

Table 3 Geometric parameters and their levels

Levels	Level 1	Level 2	Level 3	Level 4	Level 5
X1	16.45	17.45	18.45	19.45	20.45
X2	17.09	18.09	19.09	20.09	21.09
X3	43.00	44.00	45.00	46.00	47.00
X4	31.00	31.50	32.00	32.50	33.00
X5	1.40	1.50	1.60	1.70	1.80
X6	14.00	14.50	15.00	15.50	16.00

Next, we have to do the experiments (FEM analysis) and record the results of each of the 25 tests in Table 4 for both AF and ST. The results are according to Table 5.

At this stage, it is necessary to implement the Taguchi algorithm separately for each of the dependent variables AF and ST and obtain the results. Due to the nature of the dependent variables, the signal to noise ratio (S/N Ratio) function is considered *larger is better* for AF and *smaller is better* for ST. The S/N values for AF are shown in

$$AF = -984.4 + 6.32X1 - 4.05X2 + 27.97X3 + 12.69X4 + 122.5X5 + 0.0980X2 \times X2 - 0.2466X3 \times X3 - 0.1923X4 \times X4 - 19.68X5 \times X5 - 0.1477X1 \times X4 - 0.0924X2 \times X3 + 0.1289X2 \times X4 - 1.243X3 \times X5 \tag{21}$$

Table 6 and its diagram in Fig. 7, as well as the S/N values for ST in Table 6 and its diagram in Fig. 8.

According to Table 6 and DELTA values for the levels of independent variables, at this stage we cannot assume any variable from AF or ST completely noisy and completely remove it, so we leave this to the regression steps. The next step is to obtain a mathematical model of the problem using regression. As explained in the proposed algorithm, for each of the dependent variables AF and ST, we first use the SLR and then the SWLR, then FQMLR and therefore BFQMLR. Since SWLR and BFQMLR are complementary regression functions and are better than SLR and FQMLR, respectively, we provide the results for SWLR and BFQMLR only. The SWLR equation for AF is as (1), the BFQMLR for AF is as (2), and the BFQMLR, SWLR for ST are both identical and consistent with 3 (Table 7).

$$AF = -97.4 + 1.6704X1 - 0.3040X2 + 2.0632X3 + 3.916X5 \tag{20}$$

Table 4 DOE based on Taguchi L25

Run Order	X1	X2	X3	X4	X5	X6
1	16.45	17.09	43.00	31.00	1.40	14.00
2	16.45	18.09	44.00	31.50	1.50	14.50
3	16.45	19.09	45.00	32.00	1.60	15.00
4	16.45	20.09	46.00	32.50	1.70	15.50
5	16.45	21.09	47.00	33.00	1.80	16.00
6	17.45	17.09	44.00	32.00	1.70	16.00
7	17.45	18.09	45.00	32.50	1.80	14.00
8	17.45	19.09	46.00	33.00	1.40	14.50
9	17.45	20.09	47.00	31.00	1.50	15.00
10	17.45	21.09	43.00	31.50	1.60	15.50
11	18.45	17.09	45.00	33.00	1.50	15.50
12	18.45	18.09	46.00	31.00	1.60	16.00
13	18.45	19.09	47.00	31.50	1.70	14.00
14	18.45	20.09	43.00	32.00	1.80	14.50
15	18.45	21.09	44.00	32.50	1.40	15.00
16	19.45	17.09	46.00	31.50	1.80	15.00
17	19.45	18.09	47.00	32.00	1.40	15.50
18	19.45	19.09	43.00	32.50	1.50	16.00
19	19.45	20.09	44.00	33.00	1.60	14.00
20	19.45	21.09	45.00	31.00	1.70	14.50
21	20.45	17.09	47.00	32.50	1.60	14.50
22	20.45	18.09	43.00	33.00	1.70	15.00
23	20.45	19.09	44.00	31.00	1.80	15.50
24	20.45	20.09	45.00	31.50	1.40	16.00
25	20.45	21.09	46.00	32.00	1.50	14.00

$$St = 536.7 - 7.374X3 - 48.44 \times X5 \tag{22}$$

As previously stated in the description of regression methods, noisy and low-effect nerves that had a *P* value > 0.05 in ANOVA analysis were removed from the regression equation. Also, the Pareto chart of standardized effects for both AF and ST variables and each of the two modes SWLR and BFQMLR are shown in Figs. 9, 10 and 11. As can be seen, for the ST variable, due to the *P* value threshold value > 0.05, based on $\alpha = 0.15$, all nonlinear nerves (and some linear nerves) are eliminated and the SWLR and BFQMLR equations are the same. Based on ANOVA analysis, the values of R^2 , ADJUST R^2 , Prediction R^2 for each of the above modes are listed in Table 8.

Then, according to Eqs. 20, 21 and 22, the validity of each of the mathematical models was checked with the values obtained from FEM, and the relative error and RSME of each model were obtained according to Tables 9, 10, and 11. The results of these tables show that for the AF variable, the BFQMLR model has a higher R^2 , which indicates a better fit of the data. In addition, for these variables, the value of $R^2(\text{adj})$, which is used to compare models with different number of terms,

indicates the considerable superiority of the BFQMLR model. Comparison of superiority in predicting results (excluding input points for Regression) is done by R^2 (pred), in which case there is a significant advantage in the BFQMLR model, as well. On the other hand, the average relative error percentage in this model is lower than SWLR. Comparison of RSME values in this case also shows the superiority of the BFMQLR model. Therefore, in general, the BFQMLR model is selected for the dependent variable AF. Regarding the ST variable, due to the similarity of the SWLR and BFQMLR models, there is no choice between the two modes, but the sum of the above shows that the AF model is more valid than the ST model. In the next step, in order to perform the optimization operation, we define a targeting function with two output components according to the system outputs as follows:

$$\text{Obj .Function : } y = [\text{AF ST}] \tag{23}$$

According to the nature of AF (large is better) and also the nature of ST (where smaller is better) and that in the optimization process we want to minimize the objective function, it is necessary to multiply the AF variable

Table 5 Results (performed experiments by FEM) based on Taguchi L25

Run Order	X1	X2	X3	X4	X5	X6	AF	St
1	16.45	17.09	43.00	31.00	1.40	14.00	17.680	146.083
2	16.45	18.09	44.00	31.50	1.50	14.50	21.600	138.475
3	16.45	19.09	45.00	32.00	1.60	15.00	24.440	126.285
4	16.45	20.09	46.00	32.50	1.70	15.50	26.060	109.753
5	16.45	21.09	47.00	33.00	1.80	16.00	26.660	95.970
6	17.45	17.09	44.00	32.00	1.70	16.00	24.780	131.053
7	17.45	18.09	45.00	32.50	1.80	14.00	26.140	120.315
8	17.45	19.09	46.00	33.00	1.40	14.50	26.380	130.318
9	17.45	20.09	47.00	31.00	1.50	15.00	27.720	114.378
10	17.45	21.09	43.00	31.50	1.60	15.50	20.620	151.440
11	18.45	17.09	45.00	33.00	1.50	15.50	27.820	135.415
12	18.45	18.09	46.00	31.00	1.60	16.00	29.360	129.018
13	18.45	19.09	47.00	31.50	1.70	14.00	30.400	107.670
14	18.45	20.09	43.00	32.00	1.80	14.50	22.840	132.618
15	18.45	21.09	44.00	32.50	1.40	15.00	23.500	147.983
16	19.45	17.09	46.00	31.50	1.80	15.00	31.900	110.195
17	19.45	18.09	47.00	32.00	1.40	15.50	31.820	129.450
18	19.45	19.09	43.00	32.50	1.50	16.00	23.060	147.110
19	19.45	20.09	44.00	33.00	1.60	14.00	26.760	125.365
20	19.45	21.09	45.00	31.00	1.70	14.50	28.460	125.073
21	20.45	17.09	47.00	32.50	1.60	14.50	35.020	118.240
22	20.45	18.09	43.00	33.00	1.70	15.00	25.740	139.480
23	20.45	19.09	44.00	31.00	1.80	15.50	28.760	122.980
24	20.45	20.09	45.00	31.50	1.40	16.00	29.000	128.215
25	20.45	21.09	46.00	32.00	1.50	14.00	31.500	119.910

Table 6 Response table for signal to noise ratios (AF), larger is better

Level	X1	X2	X3	X4	X5	X6
1	27.25	28.54	26.78	28.28	28.02	28.29
2	27.96	28.53	27.94	28.39	28.33	28.45
3	28.50	28.46	28.67	28.57	28.57	28.47
4	29.00	28.43	29.23	28.45	28.63	28.54
5	29.50	28.26	29.59	28.52	28.66	28.45
Delta	2.25	0.28	2.82	0.28	0.64	0.25
Rank	2	5	1	4	3	6

by a negative, so the objective function is modified as follows:

$$\text{Obj. function} : y = [-AF \quad ST] \quad (24)$$

where the values of AF and ST are determined according to Eqs. 2 and 3, respectively. The upper bound and lower bound values of each independent variable (input) are determined according to level1 and level5 of each. The settings of the other parameters of the NSGA-II algorithm are as shown in Table 12. After executing the target function with the above parameters in MATLAB software version R2013a with 50-point optimal Pareto front, the optimal

Pareto front diagram and the optimal points on it are according to Table 13 and Fig. 12.

Obviously, each of the points on the optimal Pareto front can be used as an optimal point, but if we want to have only one optimal point as the final answer, as stated in the section on optimization description (4.3), we use AHP method and create a pairwise comparison table and then ask an expert user to compare the AF and ST parameters in terms of importance (for a specific application) and fill in a table according to Table 14. In Table 14, for example, the importance of AF relative to ST is three to one. It is also noteworthy that in order to combine the

Fig. 7 Main effects plot for S/N ratio (AF), larger is better

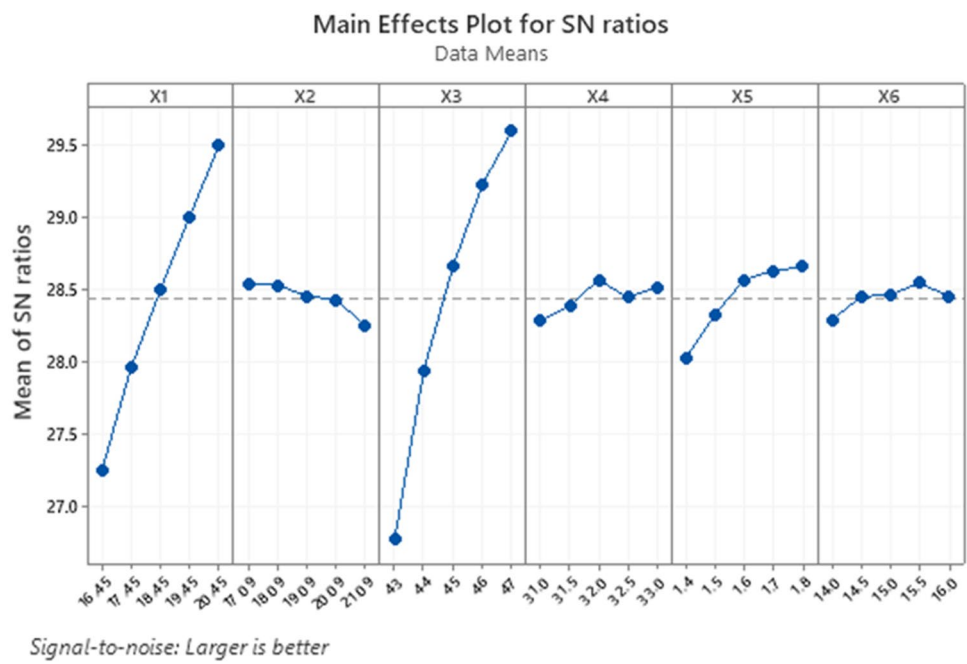


Fig. 8 Main effects plot for S/N ratio (St), smaller is better

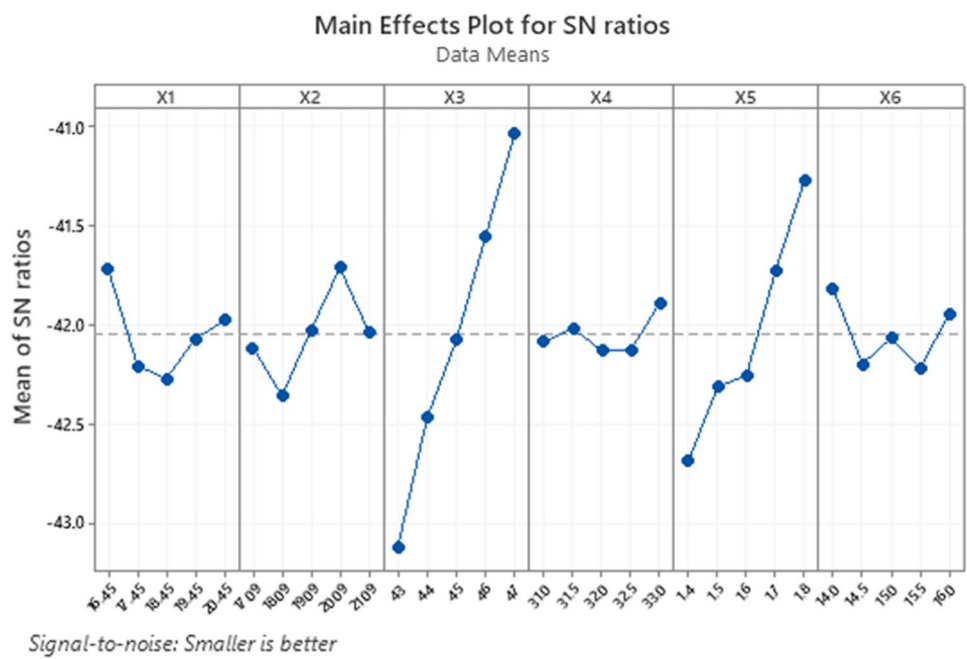


Table 7 Response table for signal to noise ratios (St), smaller is better

Level	X1	X2	X3	X4	X5	X6
1	-41.72	-42.11	-43.12	-42.08	-42.68	-41.82
2	-42.21	-42.36	-42.47	-42.02	-42.31	-42.20
3	-42.27	-42.02	-42.07	-42.13	-42.25	-42.07
4	-42.07	-41.71	-41.55	-42.13	-41.73	-42.22
5	-41.98	-42.03	-41.03	-41.89	-41.27	-41.94
Delta	0.55	0.65	2.09	0.24	1.41	0.40
Rank	4	3	1	6	2	5

Fig. 9 Pareto chart of standardized effects for SWLR of AF (only for terms which P value < 0.05 . Here 1.50 is threshold)

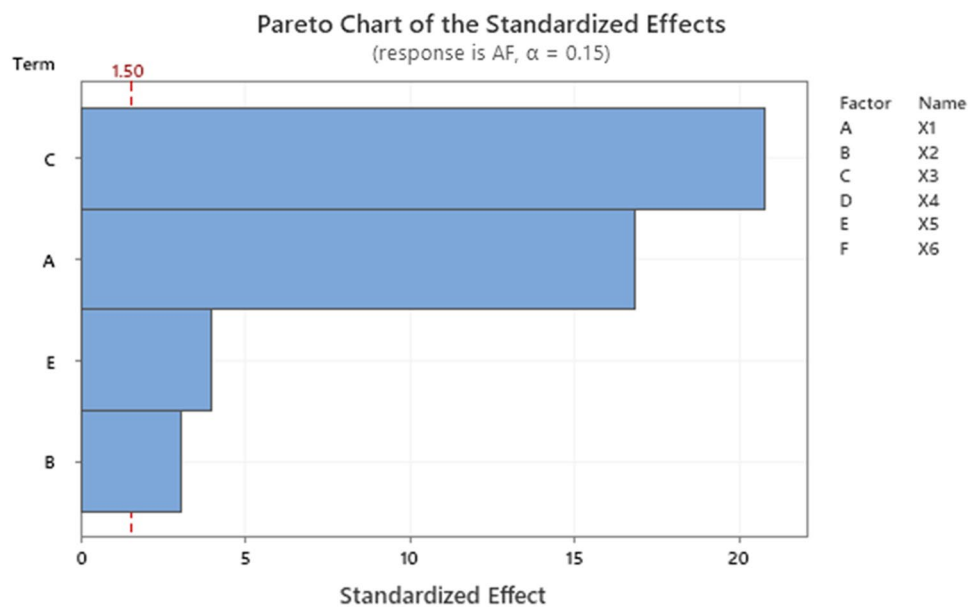
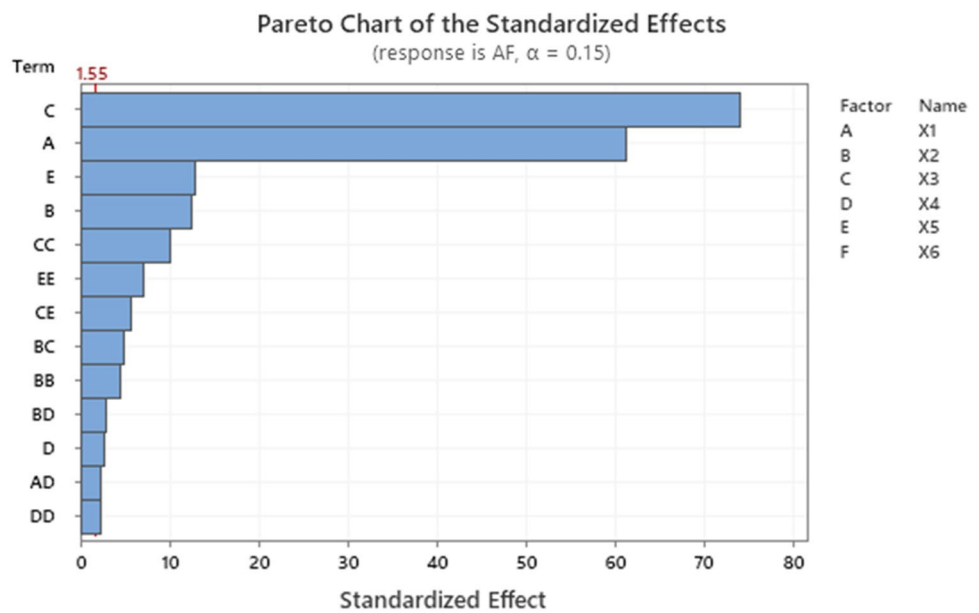


Fig. 10 Pareto chart of standardized effects for BFQMLR of AF (only for terms which P value < 0.05 . Here 1.55 is threshold)



output components according to the obtained weights, it is necessary for both of these components to be normalized before multiplying by the weights. For example, to normalize AF with respect to the optimal Pareto-front, we do the following:

$$AF_N = \frac{AF}{AF_{max} - AF_{min}} \tag{25}$$

where AF_N is the normalized value of AF and AF_{max} and AF_{min} are the maximum and minimum values for AF in the optimal Pareto-front, respectively. After performing these

steps, the table of values of the optimization parameter will be as in Table 15. The values in $Y_c =$ combined output are obtained by the following formula:

$$Y_c = W_{N_1} AF_N + W_{N_2} ST_N \tag{26}$$

As can be seen, the maximum value of the combined output in Table 15 is 1.00359 and corresponds to the point $ST = 104.729$ $AF = 34.933$, the values of its independent variables on the optimal Pareto-front are as follows:

Fig. 11 Pareto chart of standardized effects for both SWLR and BFQMLR of St (only for terms which *P* value < 0.05. Here 1.50 is threshold)

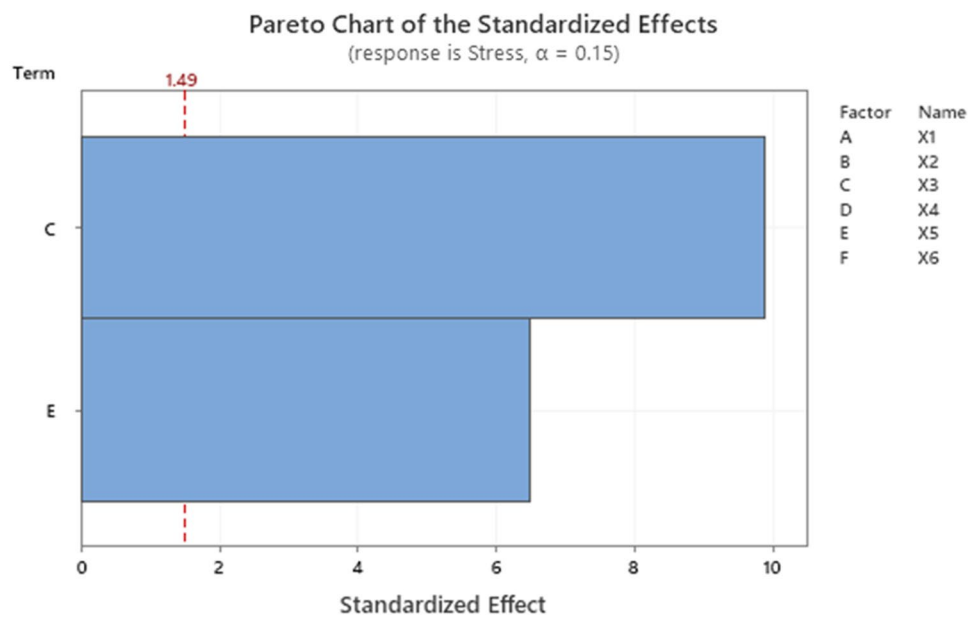


Table 8 Results of ANOVA for R^2 , R^2 (Adj.) and R^2 (Pred.)

Variable	Regression type	R^2 (%)	R^2 (Adj.) (%)	R^2 (Pred.) (%)
AF	SWLR	97.37	96.85	95.42
AF	BFQMLR	99.93	99.84	99.58
St	SWLR	86.43	85.20	82.45
St	BFQMLR	86.43	85.20	82.45

$$X1 = 20.45 \quad X3 = 47.00 \quad X5 = 1.76$$

$$X2 = 17.09 \quad X4 = 31.00 \quad X6 = 14.47$$

To show the flexibility of the above method, the above point (p3) along with the optimal points obtained for the AF to ST ratios of 4 to 1 (p4) and 8 to 1 (p8) are shown in Fig. 13.

5 Discussion

As shown in Table 6 and Fig. 8, the input variables X3 and X1 have a very strong effect on the AF output parameter, while the effect of other variables is less in this case. In addition, the effect of these two variables has a definite upward trend, while the other 4 variables fluctuate. Regarding ST output, it can be concluded from Table 7 and Fig. 9 that X3 and X5 are the most effective factors and other variables have noise effect. This effect is to

the extent that the X3 and X5 regression models are expected to be more important than the other inputs. In the mathematical model of the AF variable, according to the SWLR method, all neurons that had a *p* value > 0.05 were removed, and as a result, only 4 variables X1, X2, X3, X5 were present, and the effect of X4, X6 noise was identified and removed. Also, in the AF mathematical model based on BFQMLR, in the linear part similar to the SWLR model, only 4 variables X1, X2, X3, X5 are present. Out of 6 square terms (x_i^2), only x_2^2 , x_3^2 , x_4^2 and x_5^2 are present and other cases have a noise effect. Also, out of 30 possible terms for the interactional component, only x_3x_5 , x_2x_4 , x_2x_3 and x_1x_4 are present, and the other 26 terms have a noise effect and have been removed from the model. On the other hand, in the ST mathematical model with BFQMLR method, there are only 2 linear terms that are due to the variables X3, X5 and other linear terms with all interactional square terms have a noise effect and have been removed, so SWLR regression models, BFQMLR are the same for ST. Comparison of the effects of ANOVA analysis between the two regression models expressed for AF, as mentioned in the Results section, shows the absolute superiority of the BFQMLR model. Validity check performed on the presented regression models and the error values entered for each in Table 12 and 13 indicate the validity of all 3 regression models. Of course, the validity of this model is fully verifiable if it is valid for points other than the points used to

Table 9 Validity check for regression models of AF

Run Order	X1	X2	X3	X4	X5	X6	AF(FEM)	AF (BFQMLR)	Rel. Error %	AF (SWLR)	Rel. Error %
1	16.45	17.09	43.00	31.00	1.40	14.00	17.680	17.479	1.138	19.084	7.943
2	16.45	18.09	44.00	31.50	1.50	14.50	21.600	21.363	1.099	21.235	1.690
3	16.45	19.09	45.00	32.00	1.60	15.00	24.440	24.155	1.166	23.386	4.313
4	16.45	20.09	46.00	32.50	1.70	15.50	26.060	25.856	0.783	25.537	2.008
5	16.45	21.09	47.00	33.00	1.80	16.00	26.660	26.466	0.729	27.687	3.854
6	17.45	17.09	44.00	32.00	1.70	16.00	24.780	24.657	0.496	23.993	3.177
7	17.45	18.09	45.00	32.50	1.80	14.00	26.140	26.140	0.000	26.143	0.013
8	17.45	19.09	46.00	33.00	1.40	14.50	26.380	26.343	0.142	26.336	0.166
9	17.45	20.09	47.00	31.00	1.50	15.00	27.720	27.487	0.842	28.487	2.767
10	17.45	21.09	43.00	31.50	1.60	15.50	20.620	20.482	0.671	20.322	1.446
11	18.45	17.09	45.00	33.00	1.50	15.50	27.820	27.531	1.037	26.943	3.152
12	18.45	18.09	46.00	31.00	1.60	16.00	29.360	29.471	0.379	29.094	0.907
13	18.45	19.09	47.00	31.50	1.70	14.00	30.400	30.210	0.625	31.245	2.778
14	18.45	20.09	43.00	32.00	1.80	14.50	22.840	22.676	0.716	23.079	1.048
15	18.45	21.09	44.00	32.50	1.40	15.00	23.500	23.350	0.639	23.272	0.969
16	19.45	17.09	46.00	31.50	1.80	15.00	31.900	31.753	0.462	31.851	0.152
17	19.45	18.09	47.00	32.00	1.40	15.50	31.820	31.615	0.646	32.044	0.705
18	19.45	19.09	43.00	32.50	1.50	16.00	23.060	23.035	0.110	23.879	3.552
19	19.45	20.09	44.00	33.00	1.60	14.00	26.760	26.420	1.270	26.030	2.729
20	19.45	21.09	45.00	31.00	1.70	14.50	28.460	28.385	0.264	28.181	0.982
21	20.45	17.09	47.00	32.50	1.60	14.50	35.020	34.771	0.710	34.802	0.623
22	20.45	18.09	43.00	33.00	1.70	15.00	25.740	25.663	0.298	26.637	3.483
23	20.45	19.09	44.00	31.00	1.80	15.50	28.760	28.424	1.169	28.787	0.095
24	20.45	20.09	45.00	31.50	1.40	16.00	29.000	28.756	0.841	28.980	0.068
25	20.45	21.09	46.00	32.00	1.50	14.00	31.500	31.397	0.326	31.131	1.171
						Average	26.721	26.555	0.662	26.727	1.992
						Max	35.020	34.771	1.270	34.802	7.943
						Min	17.680	17.479	0.000	19.084	0.013

build the model. In terms of analysis of variance, such validation is performed using the parameter $R^2(\text{pred.})$, Which has an acceptable value for all 3 models according to Table 10. The optimal Pareto front shown in Fig. 12 indicates that achieving higher AF magnitudes (which is desirable) has the unintended effect of increasing stress. For this purpose, it is necessary to compromise between the values of AF and ST, which is a kind of technical contradiction, in a reliable and systematic way. For this purpose, and instead of manual weighting, which is a common method in these cases, the matrix of pairwise comparisons and determination and normalization of the weight of each output using the Analytic Hierarchy Process (AHP) has been used. The results shown in Fig. 13 confirm this claim and its conformity with the logic of the problem.s

Finally, Table 16 compares the proposed algorithm with the previous ones (mentioned in the literature review). This comparison is made in 4 contexts. In the fourth column, comparisons are made from the perspective of data collection methods, and as can be seen, some studies have used estimates based on analytical relationships or arbitrary finite points, which certainly do not provide reliable coverage of the range of inputs and their optimal point may be a local extreme. Of course, this is not the case when well-known design of experiments methods such as Taguchi orthogonal arrays or Response Surface Method (RSM) are used. In the fifth column, the optimization methods used are compared, all of which are multi-objective and each has its advantages and disadvantages. Therefore, in this case, neither can be superior to the other. In the sixth column, the methods for selecting the optimal point

Table 10 Validity check for regression models of St

Run order	X1	X2	X3	X4	X5	X6	St (FEM)	St (SWLR, BFQMLR)	Rel. Error %
1	16.45	17.09	43.00	31.00	1.40	14.00	146.083	151.802	3.915
2	16.45	18.09	44.00	31.50	1.50	14.50	138.475	139.584	0.801
3	16.45	19.09	45.00	32.00	1.60	15.00	126.285	127.366	0.856
4	16.45	20.09	46.00	32.50	1.70	15.50	109.753	115.148	4.916
5	16.45	21.09	47.00	33.00	1.80	16.00	95.970	102.930	7.252
6	17.45	17.09	44.00	32.00	1.70	16.00	131.053	129.896	0.882
7	17.45	18.09	45.00	32.50	1.80	14.00	120.315	117.678	2.192
8	17.45	19.09	46.00	33.00	1.40	14.50	130.318	129.680	0.489
9	17.45	20.09	47.00	31.00	1.50	15.00	114.378	117.462	2.697
10	17.45	21.09	43.00	31.50	1.60	15.50	151.440	142.114	6.158
11	18.45	17.09	45.00	33.00	1.50	15.50	135.415	132.210	2.367
12	18.45	18.09	46.00	31.00	1.60	16.00	129.018	119.992	6.996
13	18.45	19.09	47.00	31.50	1.70	14.00	107.670	107.774	0.097
14	18.45	20.09	43.00	32.00	1.80	14.50	132.618	132.426	0.144
15	18.45	21.09	44.00	32.50	1.40	15.00	147.983	144.428	2.402
16	19.45	17.09	46.00	31.50	1.80	15.00	110.195	110.304	0.099
17	19.45	18.09	47.00	32.00	1.40	15.50	129.450	122.306	5.519
18	19.45	19.09	43.00	32.50	1.50	16.00	147.110	146.958	0.103
19	19.45	20.09	44.00	33.00	1.60	14.00	125.365	134.740	7.478
20	19.45	21.09	45.00	31.00	1.70	14.50	125.073	122.522	2.039
21	20.45	17.09	47.00	32.50	1.60	14.50	118.240	112.618	4.755
22	20.45	18.09	43.00	33.00	1.70	15.00	139.480	137.270	1.584
23	20.45	19.09	44.00	31.00	1.80	15.50	122.980	125.052	1.685
24	20.45	20.09	45.00	31.50	1.40	16.00	128.215	137.054	6.894
25	20.45	21.09	46.00	32.00	1.50	14.00	119.910	124.836	4.108
						Average	127.31	127.366	3.057
						Max	151.440	151.802	7.478
						Min	95.970	102.930	0.097

Table 11 RSME for AF and St

Variable	Regression Type	RSME
AF	SWLR	0.627
AF	BFQMLR	0.196
St	SWLR	4.943
St	BFQMLR	4.943

Table 12 Type and value for NSGA-II parameters

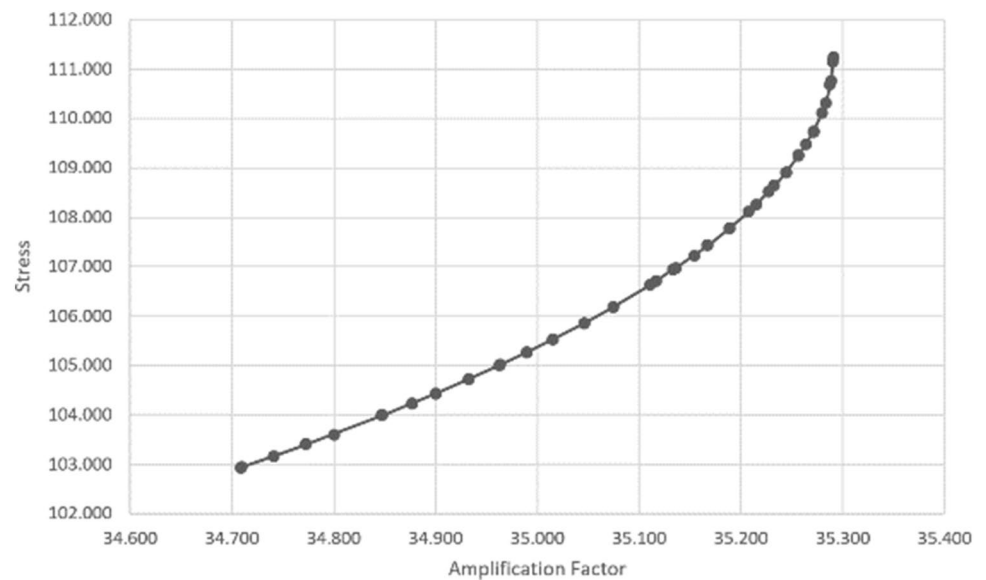
Parameter	Type	Value
Cross over	Simulated binary	0.9
Selection	Non dominated sorting and crowding distance	–
Mutation	–	0.1666
Max. no. of generations	–	500
Population size	–	100
Function tolerance	–	0.0001

from the set of answers are examined, and as can be seen, except for the proposed algorithm of this research, none of the previous cases provides such an answer and limited to a maximum of 5 optimal points (Whose choice was also unsystematic). This can be a measure of the flexibility of the algorithm for different applications of microgrippers and presented in the sixth column.

For a better understanding, if each algorithm has an advantage in a specific aspect, it is highlighted in the corresponding column, and as can be seen, the only algorithm that has an advantage in all four areas at the same time is the algorithm proposed in this paper.

Table 13 Points of optimal Pareto-front

X1	X2	X3	X4	X5	X6	AF	St
20.45	17.09	47.00	31.00	1.76	14.47	34.962	105.006
20.45	17.09	47.00	31.00	1.77	14.52	34.876	104.234
20.45	17.09	47.00	31.00	1.76	14.46	34.964	105.021
20.45	17.09	47.00	31.00	1.76	14.47	34.933	104.729
20.45	17.09	47.00	31.00	1.68	14.69	35.244	108.912
20.45	17.09	47.00	31.00	1.75	14.43	35.015	105.533
20.45	17.09	47.00	31.00	1.67	14.51	35.256	109.244
20.45	17.09	47.00	31.00	1.80	14.46	34.708	102.930
20.45	17.09	47.00	31.00	1.80	14.46	34.741	103.166
20.45	17.09	47.00	31.00	1.74	14.46	35.046	105.864
20.45	17.09	47.00	31.00	1.77	14.47	34.900	104.437
20.45	17.09	47.00	31.00	1.69	14.47	35.207	108.108
20.45	17.09	47.00	31.00	1.71	14.47	35.167	107.427
20.45	17.09	47.00	31.00	1.67	14.51	35.257	109.256
20.45	17.09	47.00	31.00	1.75	14.45	34.990	105.271
20.45	17.09	47.00	31.00	1.65	14.43	35.279	110.107
20.45	17.09	47.00	31.00	1.79	14.78	34.800	103.612
20.45	17.09	47.00	31.00	1.65	14.46	35.283	110.313
20.45	17.09	47.00	31.00	1.63	14.69	35.290	111.149
20.45	17.09	47.00	31.00	1.70	14.46	35.189	107.777
20.45	17.09	47.00	31.00	1.77	14.46	34.900	104.437
20.45	17.09	47.00	31.00	1.76	14.78	34.933	104.729
20.45	17.09	47.00	31.00	1.77	14.47	34.876	104.234
20.45	17.09	47.00	31.00	1.64	14.46	35.288	110.773
20.45	17.09	47.00	31.00	1.79	14.71	34.773	103.402
20.45	17.09	47.00	31.00	1.80	14.46	34.710	102.942
20.45	17.09	47.00	31.00	1.71	14.77	35.154	107.230
20.45	17.09	47.00	31.00	1.66	14.78	35.264	109.480
20.45	17.09	47.00	31.00	1.66	14.77	35.271	109.730
20.45	17.09	47.00	31.00	1.72	14.47	35.111	106.637
20.45	17.09	47.00	31.00	1.79	14.71	34.773	103.402
20.45	17.09	47.00	31.00	1.68	14.69	35.244	108.912
20.45	17.09	47.00	31.00	1.72	14.47	35.117	106.706
20.45	17.09	47.00	31.00	1.74	14.43	35.046	105.864
20.45	17.09	47.00	31.00	1.68	14.46	35.233	108.634
20.45	17.09	47.00	31.00	1.78	14.46	34.847	103.992
20.45	17.09	47.00	31.00	1.66	14.77	35.271	109.747
20.45	17.09	47.00	31.00	1.63	14.46	35.290	111.243
20.45	17.09	47.00	31.00	1.69	14.46	35.215	108.256
20.45	17.09	47.00	31.00	1.68	14.46	35.227	108.513
20.45	17.09	47.00	31.00	1.75	14.43	35.015	105.533
20.45	17.09	47.00	31.00	1.70	14.46	35.189	107.777
20.45	17.09	47.00	31.00	1.72	14.46	35.136	106.969
20.45	17.09	47.00	31.00	1.71	14.47	35.167	107.427
20.45	17.09	47.00	31.00	1.80	14.46	34.708	102.930
20.45	17.09	47.00	31.00	1.75	14.45	34.990	105.271
20.45	17.09	47.00	31.00	1.64	14.78	35.288	110.678
20.45	17.09	47.00	31.00	1.72	14.69	35.133	106.943
20.45	17.09	47.00	31.00	1.73	14.46	35.074	106.185
20.45	17.09	47.00	31.00	1.78	14.46	34.846	103.987

Fig. 12 Optimal Pareto-front

6 Conclusions

Microgrippers are the end effectors in micro-operations and micro-manipulations, making them a sensitive instrument in terms of accuracy and efficiency. As an actuation mechanism for microgrippers, piezo-electric actuation has several benefits, but there is a major drawback; the range of motion in this type of actuation is minimal. Therefore, amplification mechanisms are of great interest, especially in piezo-electric microgrippers. Amplification Factor is an important parameter to ensure a great range of motion for the gripper, thus resulting in a wider application use. Using four stages of amplification, we achieved a desirable range of motion for the microgripper. This paper proposed a novel optimization process to adjust a symmetric compliant piezoelectric actuated microgripper for specific applications. A trade-off was made between the displacement amplification factor and maximum generated mechanical stress using multi-objective optimization. Based on

the optimization, a set of designs was proposed instead of a single optimum design. A selection method based on the Analytical Hierarchy Process (AHP) was suggested for the selection process of designs for specific applications. The performance of the proposed microgripper design was inspected using the finite element method. Taguchi's method of designing experiments was used to identify effective variables and obtain relations between design parameters and intended responses. Using NSGA-II instead of the traditional Multi-Objective Genetic Algorithm (MOGA) reduces the complexity of calculations, speeds up the algorithm, leads to easier elitism, and preserves the GA population's diversity, leading to more accurate and faster results. Also, using the AHP algorithm prevents possible errors in the final decision of the designer.

Table 14 Pairwise compare of output components (AF vs. St) based on AHP

Compare	AF	St	W	W _n
AF	1	3	1.732	0.750
St	0.333	1	0.577	0.250

Table 15 Combined output using normalized weights

AF	St	Combined	AF	St	Combined
34.708	102.930	1.00243	35.117	106.706	1.00219
34.708	102.930	1.00243	35.133	106.943	1.00179
34.710	102.942	1.00244	35.136	106.969	1.00179
34.741	103.166	1.00271	35.154	107.230	1.00134
34.773	103.402	1.00296	35.167	107.427	1.00098
34.773	103.402	1.00296	35.167	107.427	1.00098
34.800	103.612	1.00314	35.189	107.777	1.00026
34.846	103.987	1.00338	35.189	107.777	1.00026
34.847	103.992	1.00339	35.207	108.108	0.99949
34.876	104.234	1.00350	35.215	108.256	0.99913
34.876	104.234	1.00350	35.227	108.513	0.99845
34.900	104.437	1.00356	35.233	108.634	0.99812
34.900	104.437	1.00356	35.244	108.912	0.99731
34.933	104.729	1.00359	35.244	108.912	0.99731
34.933	104.729	1.00359	35.256	109.244	0.99628
34.962	105.006	1.00356	35.257	109.256	0.99624
34.964	105.021	1.00356	35.264	109.480	0.99549
34.990	105.271	1.00348	35.271	109.730	0.99462
34.990	105.271	1.00348	35.271	109.747	0.99456
35.015	105.533	1.00336	35.279	110.107	0.99321
35.015	105.533	1.00336	35.283	110.313	0.99240
35.046	105.864	1.00313	35.288	110.678	0.99089
35.046	105.864	1.00313	35.288	110.773	0.99048
35.074	106.185	1.00283	35.290	111.149	0.98881
35.111	106.637	1.00228	35.290	111.243	0.98837

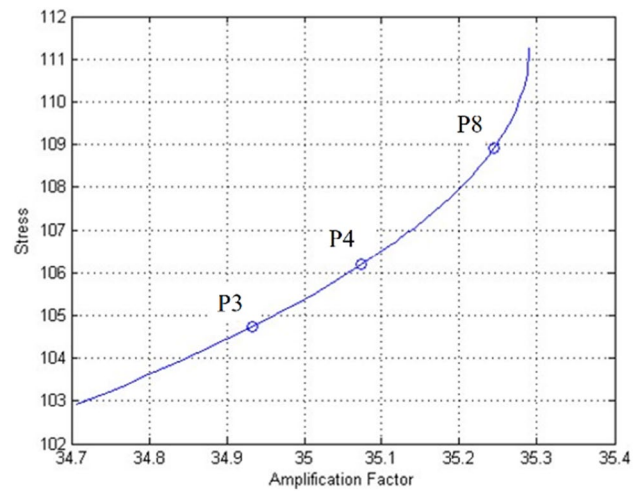


Fig. 13 Combined output points on the optimal Pareto-front

Table 16 Comparison of the proposed algorithm with previous ones

No	Author (s)	Optimization method (multi/single)	Year	Data gathering method	Selection method for the optimum point	Special application/general purpose
1	Grossard, M. et al	Multi Obj. GA	2009	Estimation using simplification of the analytical relationships	5 Discrete points (no selection plan)	Special application
2	5 Discrete Points (No Selection Plan)	Multi Obj. GA	2011	Estimation using simplification of the analytical relationships	Xiao, S., Li, Y. and Zhao, X	Special Application
3	Dao et al	Multi Obj. Differential evolution (DE)	2017	Discrete arbitrary points	Discrete points (no selection plan)	Special application
4	Ho et al	Multi Obj. HTBLO	2019	Taguchi orthogonal arrays	3 Case studies (no selection plan)	Special application
5	Ho et al	Multi Obj Jaya Algorithm	2019	Taguchi orthogonal arrays	A Single optimum point (no selection plan)	Special application
6	Nguyen, D.N., et al	Multi Obj. GA	2019	Response surface method	5 Discrete points (no selection plan)	Special application
7	Das, T.K., et al	Multi Obj mixed-integer sequential quadratic programming	2021	Response Surface Method	A Single optimum point (no selection plan)	Special application
8	This Study	Multi Obj. GA	2022	Taguchi orthogonal arrays	An optimal pareto front	General purpose

Author contribution All of the authors of this manuscript confirm that this work is original and has not been published elsewhere nor is it currently under consideration for publication elsewhere. They confirm that the manuscript has been read and approved by all named authors and that there are no other persons who satisfied the criteria for authorship but are not listed. The authors further confirm that the order of authors listed in the manuscript has been approved by all of them.

Funding They state that no funds, grants or other financial support were received for conducting this study and have no relevant financial or non-financial interests to disclose.

Declarations

Conflict of interest The Authors declare that there is no conflict of interest.

Open Access This article is licensed under a Creative Commons Attribution 4.0 International License, which permits use, sharing, adaptation, distribution and reproduction in any medium or format, as long as you give appropriate credit to the original author(s) and the source, provide a link to the Creative Commons licence, and indicate if changes were made. The images or other third party material in this article are included in the article's Creative Commons licence, unless indicated otherwise in a credit line to the material. If material is not included in the article's Creative Commons licence and your intended use is not permitted by statutory regulation or exceeds the permitted use, you will need to obtain permission directly from the copyright holder. To view a copy of this licence, visit <http://creativecommons.org/licenses/by/4.0/>.

References

- Esposito D et al (2019) A neuromorphic model to match the spiking activity of Merkel mechanoreceptors with biomimetic tactile sensors for bioengineering applications. *IEEE Trans Med Robot Bionics* 1(2):97–105
- Gupta A, Pal P (2019) Micro-electro-mechanical system-based drug delivery devices. In: *Bioelectronics and medical devices*, 2019 Jan 1. Woodhead Publishing, pp 183–210
- Xu W et al (2020) 2D MEMS-based multilayer Laue lens nanofocusing optics for high-resolution hard x-ray microscopy. *Opt Express* 28(12):17660–17671
- Javed Y, Mansoor M, Shah IA (2019) A review of principles of MEMS pressure sensing with its aerospace applications. *Sens Rev* 39:652–654
- Liang C et al (2018) Design and control of a novel asymmetrical piezoelectric actuated microgripper for micromanipulation. *Sens Actuators A* 269:227–237
- Potekhina A et al (2021) Design and characterization of a polymer electrothermal microgripper with a polynomial flexure for efficient operation and studies of moisture effect on negative deflection. *Microsyst Technol* 27(7):2723–2731
- Fard-Vatan HM, Hamed M (2020) Design, analysis and fabrication of a novel hybrid electrothermal microgripper in microassembly cell. *Microelectr En* 231:111374
- Velosa-Moncada LA et al (2018) Design of a novel MEMS microgripper with rotatory electrostatic comb-drive actuators for biomedical applications. *Sensors* 18(5):1664
- Choi A, Gultepe E, Gracias DH (2017) Pneumatic delivery of untethered microgrippers for minimally invasive biopsy. In: 2017 13th IEEE international conference on control and automation (ICCA). IEEE

10. Zhang J et al (2017) Reliable grasping of three-dimensional untethered mobile magnetic microgripper for autonomous pick-and-place. *IEEE Robot Autom Lett* 2(2):835–840
11. Llewellyn-Evans H, Griffiths C, Fahmy A (2020) Design process and simulation testing of a shape memory alloy actuated robotic microgripper. *Microsyst Technol* 26(3):885–900
12. Mehrabi H, Aminzahed I (2020) Design and testing of a micro-gripper with SMA actuator for manipulation of micro components. *Microsyst Technol* 26(2):531–536
13. Mehrabi H, Hamed M, Aminzahed I (2020) A novel design and fabrication of a micro-gripper for manipulation of micro-scale parts actuated by a bending piezoelectric. *Microsyst Technol* 26(5):1563–1571
14. Das TK et al (2020) Characterization of a compact piezoelectric actuated microgripper based on double-stair bridge-type mechanism. *J Micro-Bio Robot* 16(1):79–92
15. Al-Jodah A et al (2020) A fuzzy disturbance observer based control approach for a novel 1-DOF micropositioning mechanism. *Mechatronics* 65:102317
16. Al-Jodah A et al (2020) Development and control of a large range XY θ micropositioning stage. *Mechatronics* 66:102343
17. Wang F et al (2014) Design of a piezoelectric-actuated micro-gripper with a three-stage flexure-based amplification. *IEEE/ASME Trans Mechatron* 20(5):2205–2213
18. Sun X et al (2013) A novel flexure-based microgripper with double amplification mechanisms for micro/nano manipulation. *Rev Sci Instrum* 84(8):085002
19. Chen X et al (2020) Design of a compliant mechanism based four-stage amplification piezoelectric-driven asymmetric micro-gripper. *Micromachines* 11(1):25
20. Dao T-P et al (2017) Analysis and optimization of a micro-displacement sensor for compliant microgripper. *Microsyst Technol* 23(12):5375–5395
21. Ho NL et al (2019) Multi-objective optimization design of a compliant microgripper based on hybrid teaching learning-based optimization algorithm. *Microsyst Technol* 25(5):2067–2083
22. Xiao S, Li Y, Zhao X (2011) Optimal design of a novel micro-gripper with completely parallel movement of gripping arms. In: 2011 IEEE 5th international conference on robotics, automation and mechatronics (RAM). IEEE
23. Ho NL et al (2019) Optimal design of a compliant micro-gripper for assemble system of cell phone vibration motor using a hybrid approach of ANFIS and Jaya. *Arab J Sci Eng* 44(2):1205–1220
24. Grossard M et al (2009) Mechanical and control-oriented design of a monolithic piezoelectric microgripper using a new topological optimization method. *IEEE/ASME Trans Mechatron* 14(1):32–45
25. Nguyen DN et al (2019) Multi-objective optimization design for a sand crab-inspired compliant microgripper. *Microsyst Technol* 25(10):3991–4009
26. Das TK et al (2021) A novel compliant piezoelectric actuated symmetric microgripper for the parasitic motion compensation. *Mechan Mach Theory* 155:104069
27. Taguchi G et al (2005) Taguchi's quality engineering handbook. Wiley, New York
28. Asiltürk I, Akkuş H (2011) Determining the effect of cutting parameters on surface roughness in hard turning using the Taguchi method. *Measurement* 44(9):1697–1704
29. Anyılmaz M (2006) Design of experiment and an application for Taguchi method in quality improvement activity. Dumlupınar University, Turkey
30. Köksoy O, Zehra Muluk F (2004) Solution to the Taguchi's S problem with correlated responses. *Gazi Univ J Sci* 17(1):59–70
31. Ball AK et al (2019) Experimentation modelling and optimization of electrohydrodynamic inkjet microfabrication approach: a Taguchi regression analysis. *Sādhanā* 44(7):1–16
32. Roy RK (2010) A primer on the Taguchi method. Society of Manufacturing Engineers, New York
33. Shetty R et al (2009) Taguchi's technique in machining of metal matrix composites. *J Braz Soc Mech Sci Eng* 31:12–20
34. Magabe R et al (2019) Modeling and optimization of Wire-EDM parameters for machining of Ni 55.8 Ti shape memory alloy using hybrid approach of Taguchi and NSGA-II. *Int J Adv Manuf Technol* 102(5):1703–1717
35. Montgomery DC (2017) Design and analysis of experiments. Wiley, New York
36. Hashemi SMB et al (2019) Statistical modeling of the inactivation of spoilage microorganisms during ohmic heating of sour orange juice. *LWT* 111:821–828
37. Prakash C et al (2016) Multi-objective optimization of powder mixed electric discharge machining parameters for fabrication of biocompatible layer on β -Ti alloy using NSGA-II coupled with Taguchi based response surface methodology. *J Mech Sci Technol* 30(9):4195–4204
38. Srinivas N, Deb K (1994) Multiobjective optimization using nondominated sorting in genetic algorithms. *Evol Comput* 2(3):221–248
39. Deb K et al (2002) A fast and elitist multiobjective genetic algorithm: NSGA-II. *IEEE Trans Evol Comput* 6(2):182–197
40. Haghsheenas Gorgani H, Jahantigh Pak A (2018) A genetic algorithm based optimization method in 3D solid reconstruction from 2D multi-view engineering drawings. *J Comput Appl Mech* 49(1):161–170
41. Maghsoudi P, Sadeghi S, Gorgani HH (2018) Comparative study and multi-objective optimization of plate-fin recuperators applied in 200 kW microturbines based on non-dominated sorting and normalization method considering recuperator effectiveness, exergy efficiency and total cost. *Int J Therm Sci* 124:50–67
42. Maghsoudi P et al (2018) A comprehensive thermo-economic analysis, optimization and ranking of different microturbine plate-fin recuperators designs employing similar and dissimilar fins on hot and cold sides with NSGA-II algorithm and DEA model. *Appl Therm Eng* 130:1090–1104
43. Gorgani HH, Pak AJ (2020) Adaptation of engineering graphics courses to modern design approaches using a hybrid data mining method based on QFD and fuzzy dematel. *Majallah-i Amuzih-i Muhandisi-i Iran* 22(86):55–64

Publisher's Note Springer Nature remains neutral with regard to jurisdictional claims in published maps and institutional affiliations.